



Detection of Mo geochemical anomaly in depth using a new scenario based on spectrum–area fractal analysis

H. Mahdianfar

Department of Mining Engineering, University of Gonabad, Gonabad, Iran

Received 4 January 2019; received in revised form 6 July 2019; accepted 6 July 2019

Keywords

Power Spectrum–Area Fractal Analysis

Anomaly Separation

Principal Component Analysis

Blind Geochemical Anomaly

Pattern Recognition

Abstract

Detection of deep and hidden mineralization using the surface geochemical data is a challenging subject in the mineral exploration. In this work, a novel scenario based on the spectrum–area fractal analysis (SAFA) and the principal component analysis (PCA) has been applied to distinguish and delineate the blind and deep Mo anomaly in the Dalli Cu–Au porphyry mineralization area. The Dalli mineral deposit is located on the volcanic–plutonic belt of Sahand–Bazman in the central part of Iran. The geochemical data was transformed to the frequency domain using the Fourier transformation, and SAFA was applied for classification of geochemical frequencies and detection of geochemical populations. The very low-frequency signals in the fractal method were separated using the low-pass filter function and were interpreted using PCA. This scenario demonstrates that the Mo element has an important role in the mineralization phase in the very low-frequency signals that are related to the deep mineralization; it is an important innovation in this work. Then the Mo geochemical anomaly has been mapped using the inverse Fourier transformation. This research work shows that the high-power spectrum values in SAFA are related to the background elements and the deep mineralization. Two exploratory boreholes drilled inside and outside the deep Mo anomaly area properly confirm the results of the proposed approach.

1. Introduction

The interpretation of geochemical data has generally been performed in the spatial domain. Some of these frequent methods in the spatial domain consist of the mineral potential mapping [1-5], factor analysis [6, 7], and fractal methods [8-11]. The geochemical data has been analyzed in the spatial domain more than the frequency domain (FD). The frequency characteristics of geochemical processes have been considered for determination of anomaly and background [12-16]. The spectral analysis has been widely used for data processing and pattern recognition in the geosciences [17]. There is a relationship between the geochemical frequency signals and

the deep geochemical anomaly [15, 18-20]. The geochemical background and the deep mineral deposits can create the low-frequency geochemical signals in the surface. The deep mineralized and non-mineralized zones can be distinguished using the discriminant criteria in FD.

The geochemical distribution map can be considered as different frequency signals [21]. These maps can be transferred to FD using the two dimensional-Fourier transform (2D-FT) [22, 23]. The frequency signals of geochemical data can be determined in FD. One of the equations used for conducting FT is presented bellow [24]:

$$F(K_x, K_y) = \int_{-\infty}^{\infty} \int_{-\infty}^{\infty} f(x, y) \cos(K_x x + K_y y) dx dy - i \int_{-\infty}^{\infty} \int_{-\infty}^{\infty} f(x, y) \sin(K_x x + K_y y) dx dy \quad (1)$$

where $f(x,y)$ is the initial geochemical function, and K_x and K_y are “wave numbers” in the direction of x and y axes. The real and imaginary components of the signals are $R(K_x, K_y)$ and $I(K_x, K_y)$. The power spectrum values are calculated as follow [25, 26]:

$$E(K_x, K_y) = R^2(K_x, K_y) + I^2(K_x, K_y) \quad (2)$$

The fractal method has been defined in FD by applying the spectrum-area fractal model [27].

In this work, a new combined method based on SAFA and PCA is proposed for interpretation of the surface geochemical data. The complicated geochemical populations can be decomposed using this method. Identification and detection of mineralization anomalies from the barren rocks is an essential issue in the mining exploration. This proposed method is useful for detection of the deep mineralization that may cause the weak anomaly in the surface. In this work, the SAFA-PCA method is used to identify the blind Mo geochemical anomaly in the depth based on the surface geochemical data in the Dalli mineralization area. PCA, as an important dimension reduction tool, converts the datasets to uncorrelated factors [16]. The PCA method is commonly utilized for interpretation of data in the geoscience field [28-34].

2. Materials and methods

2.1. Studied area

The Dali Cu-Au porphyry mineralization area is located in the Urmieh-Dokhtar intrusive-volcanic belt in Iran [35, 36]. The mineralization of copper and gold is shown in the igneous diorite, quartz diorite porphyry, and porphyritic amphibole andesite, andesite, dacite, and pyroclastic in this area (Figure 1) [37]. The volcanic and pyroclastic rocks are related to the Miocene volcanic rocks and are disposed with a length of 30 km in the north-north east direction.

In the north part of the area, mineralization is shown in the andesite, quartz diorite, and granodiorite rocks. The potassic alteration is more shown in the central part of the area, has occurred in the tonalitic rocks, and consists of the mineralization of quartz, magnetite, and biotite. The sericite, sericite-chlorite, and propylitic-potassic alterations are located around the potassic alteration. In the diorite and andesite rocks, the copper and gold mineralizations are more located in the alterations of potassic-phyllitic and propylitic-silicic [36, 37].

2.2. Spectrum–area fractal analysis (SAFA)

Various fractal methods have been used for interpretation of geochemical data [38]. SAFA is a new method that has been applied in the frequency domain of geochemical data. SAFA illustrates the relationships between the areas of different frequency signals in the power spectrum distribution map and the spectral energy density above $S[A(>S)]$ on 2D-FT, and for a 2D linear case gives:

$$A(\geq S) \propto S^{-2/\beta} \quad (3)$$

β is the anisotropic scaling exponent [16]. The power-law relationships in the spatial and frequency domains are powerful tools for anomaly separation in the geochemistry according to the distinctive generalized self-similarity [39-42]. SAFA has been applied for elimination of the very low-frequency signals as the background factor from the anomaly factor [16, 22, 27, 43-46]. SAFA is performed as bellow:

(1) The interpolation of the surface geochemical data in the spatial domain. (2) The transformation of geochemical data in the spatial domain to FD using 2D-FT. (3) The delineation of the SAFA plot (the power spectrum values versus the area with the log-log scaling). Several populations are distinguished based on the straight lines that can be fitted on the SAFA plot. The higher cut-off value separates the signals with the high-power spectrum values from the other frequencies. The obtained frequency class based on this cut-off value is related to the background and the deep mineralization elements. This fact was demonstrated properly in this research work.

3. Discussion

A grid net of $50 \times 50 \text{ m}^2$ was utilized for the systematic soil sampling. 165 samples with the size fraction of -200 mesh were collected and analyzed for 30 elements using the ICP-MS method in this area. The geochemical distribution maps of 30 elements in the spatial domain of geochemical data were transferred to the frequency domain using 2D-FT. The 2D distribution map of the power spectrum values versus the wave numbers in the vertical and horizontal directions for Cu and Mo is illustrated in Figure 2.

The wave number values in the center of this image are zero.

SAFA was performed on the power spectrum distribution map of Cu, and three straight lines were fitted on the fractal diagram based on the

least-square regression (Figure 3). The area A(S) is equal to the number of cells (multiplied by the cell area) with the power spectrum values greater than S. The power spectrum value is increased towards the right, and accordingly, the area is decreased. The geochemical populations are defined by the breakpoints and the different line segments in this log-log plot. Accordingly, there are three populations in the Cu power spectrum data. The first and second Cu thresholds are 12.3 and 13.95, respectively. The right-hand straight

line presents the low-frequency signals with the power spectrum values more than $10^{13.95}$ and pertains to the background component and the weak surface anomalies. These weak anomalies in the surface are related to the blind and the deep ore deposit. Identifying the relationship between the geochemical frequency signals and the location of the deep ore deposit is a novel interesting achievement in the mining geochemistry.

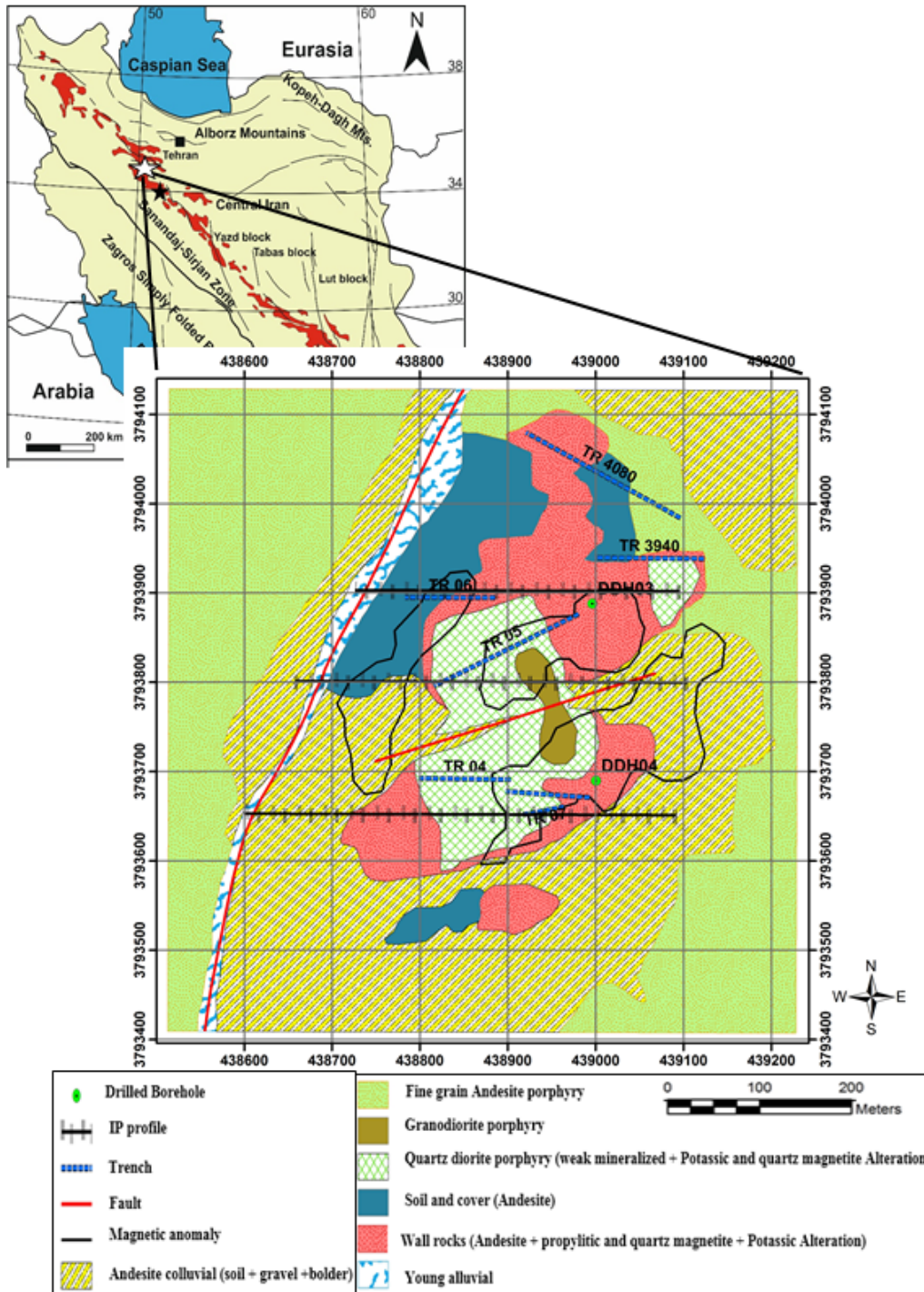


Figure 1. The geology map of studied area and the position of exploratory works [37].

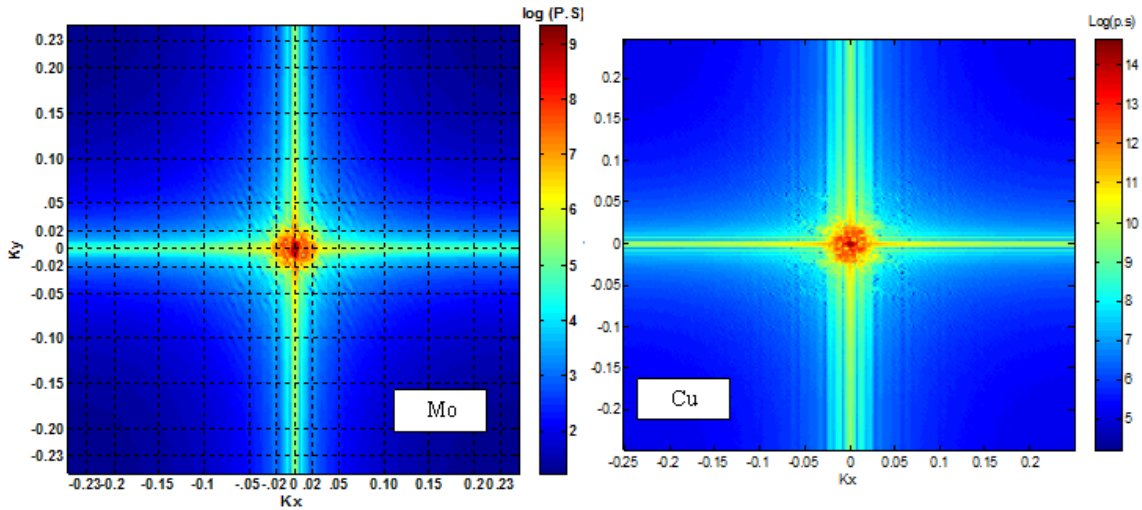


Figure 2. The power-spectrum distribution maps of Cu and Mo obtained by the Fourier transformation [18].

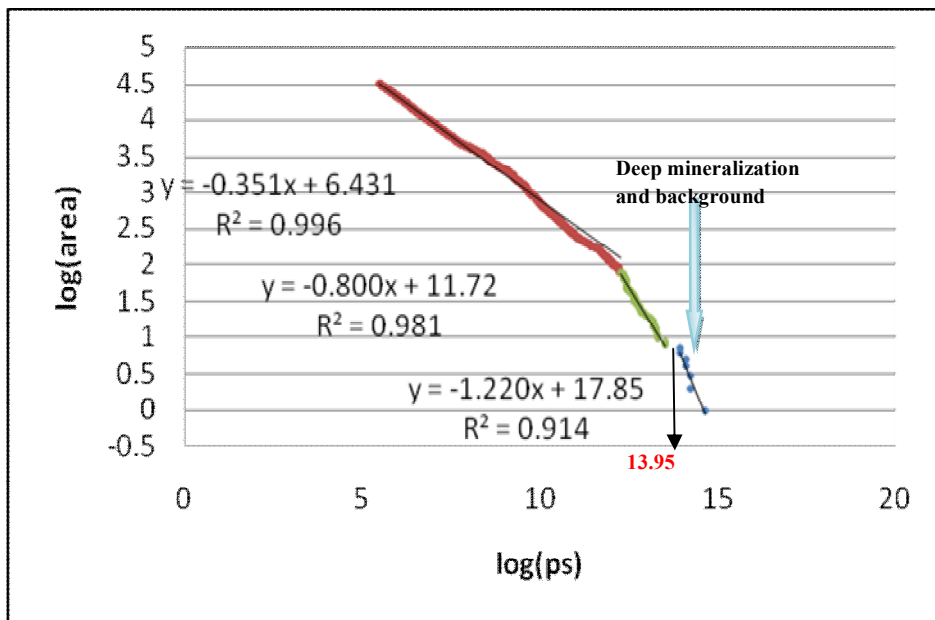


Figure 3. The log-log plot of SAFA for Cu element (logarithm of area versus logarithm of power spectrum values (PS)).

The various geochemical populations that were distinguished by SAFA can be separated using several filter functions. A low-pass filter based on the threshold of $10^{13.95}$ was performed on the power spectrum distribution map to remove the high and the moderate frequency geochemical signals. Therefore, the wave numbers with the power spectrum values more than $10^{13.95}$ were preserved and the other frequencies were removed. Detection and separation of the weak surface anomaly from the background is a major subject in the mineral exploration. The deep mineral deposits can create the weak surface anomalies with a low variability. These weak surface anomalies hold the low concentrations and consist of the low frequency signals. Some deep mineral deposits may cause very weak anomalies

in the surface. Therefore, the concentrations of mineralization elements have a low variability and may be less than the background values. This means that FD of the surface geochemical data for blind and deep geochemical anomalies consists of the low-frequency signals. Therefore, in order to detect and determine the background component and the deep mineralization factor, PCA was performed on the low-frequency signals of the elements. In this work, the SAFA-PCA scenario was successfully used for the Mo potential mapping in the depth based on the surface geochemical data. PCA, as a dimension-reduction method, reduced the 30 features (elements) to 2 components based on the low-frequency signals (Table 1 and Figure 4).

Table 1. The rotated component matrix obtained from the SAFA- PCA approach.

	Component	
	PC1 (background component)	PC2 (mineralization component)
Au	0.886	0.300
Al	0.985	0.174
As	0.976	0.219
B	0.983	0.182
Ba	0.987	0.159
Ca	0.973	0.189
Ce	0.984	0.175
Co	0.984	0.176
Cr	0.983	0.185
Cu	0.850	0.467
Fe	0.984	0.174
Ga	0.985	0.173
K	0.985	0.170
La	0.985	0.174
Li	0.984	0.176
Mg	0.985	0.170
Mn	0.983	0.184
Mo	0.101	0.989
Na	0.986	0.167
Ni	0.977	0.214
P	0.985	0.173
Pb	0.986	0.164
S	0.895	0.441
Sc	0.982	0.185
Sr	0.985	0.169
Ti	0.984	0.177
V	0.983	0.180
Y	0.985	0.173
Zn	0.986	0.168
Zr	0.979	0.201

The PCA method shows that the 29 elements such as Cu and Au have a similar treatment and exposure in the first principal component. All the 30 elements except for Mo are shown in this factor as the geochemical background component. In this low-frequency band, Mo is completely different from the other elements in the spatial and frequency behaviors. For this reason, it was separated from the other elements in the rotated component matrix and was exclusively located in the second component (Table 1 and Figure 4). These results demonstrate the interesting achievement about the situation of Mo in the depth. The second component pertains to the deep mineralization phase that is not achievable in the spatial domain of geochemical data. The deep mineralization elements cannot simply migrate to the Earth's surface. Hence, they only create the

low-frequency signals on the surface geochemical distribution map. The current research work shows that the low-frequency geochemical signals in SAFA are related to the deep mineralization elements and the background elements.

The Mo geochemical distribution map was obtained in the spatial domain based on the initial geochemical data (Figure 5). This map cannot properly show the situation of Mo anomaly. The Mo geochemical map was also obtained in FD. The potential map of the Mo mineralization in the depth was obtained using the inverse Fourier transform and the SAFA results (Figure 6). This map presents the Mo geochemical potential map in the depth. The two boreholes DDH03 and DDH04 were drilled in this area (Figure 6). The distribution of Mo concentration in the DDH03 and DDH04 boreholes is depicted in Figure 7.

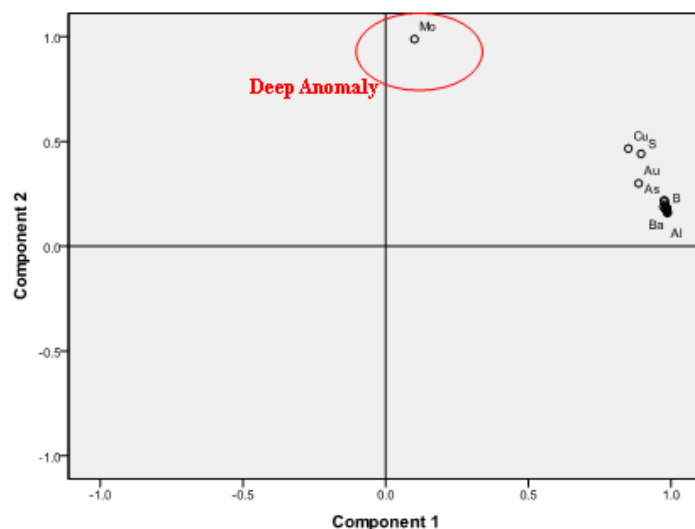


Figure 4. The component plot in rotated space using SAFA-PCA; Mo has been distinguished as the mineralization element in the depth.

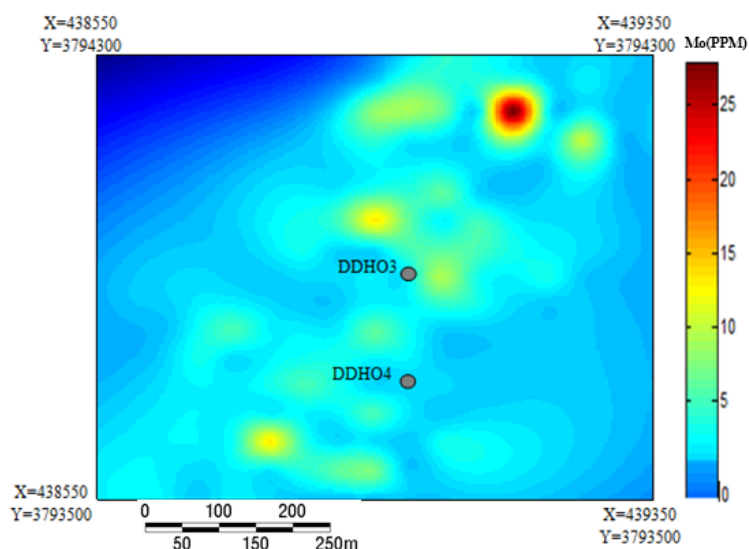


Figure 5. The Mo geochemical distribution map in the spatial domain and the position of boreholes.

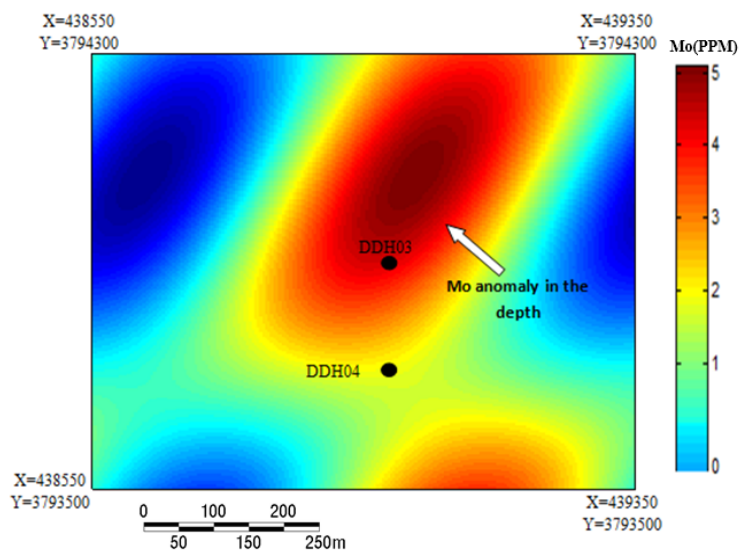


Figure 6. The Mo geochemical distribution map in the depth using the SAFA-PCA approach and the position of boreholes.

The DDH03 borehole that is located on the deep Mo anomaly area illustrates a deep mineralization zone from 270 m until 350 m, while the DDH04 borehole that drilled in the out of anomaly area lacks Mo mineralization in the depth. The geochemical information and the boreholes in this studied area confirm the results obtained by the SAFA-PCA method. The mineralization zone illustrates a trend for the enrichment of Mo towards the depth. The exploratory studies show an oxide zone near the surface and the hypogen zone in the depth in this area. The drilled boreholes show an obvious association with the Mo potential map obtained from the proposed approach. These boreholes properly demonstrate

the results of the new proposed SAFA-PCA method about the deep anomaly. The Mo anomaly map obtained from SAFA-PCA shows the exploratory information about the depth better than the spatial domain map.

The proposed hybrid method combining SAFA and PCA is an effective pattern recognition approach for decomposition of mixed geochemical populations and identification of weak surface geochemical anomalies that have been hidden within the strong geochemical background. Based on this work, the low-frequency signals obtained from SAFA consist of information about the background elements and the deep mineralization elements.

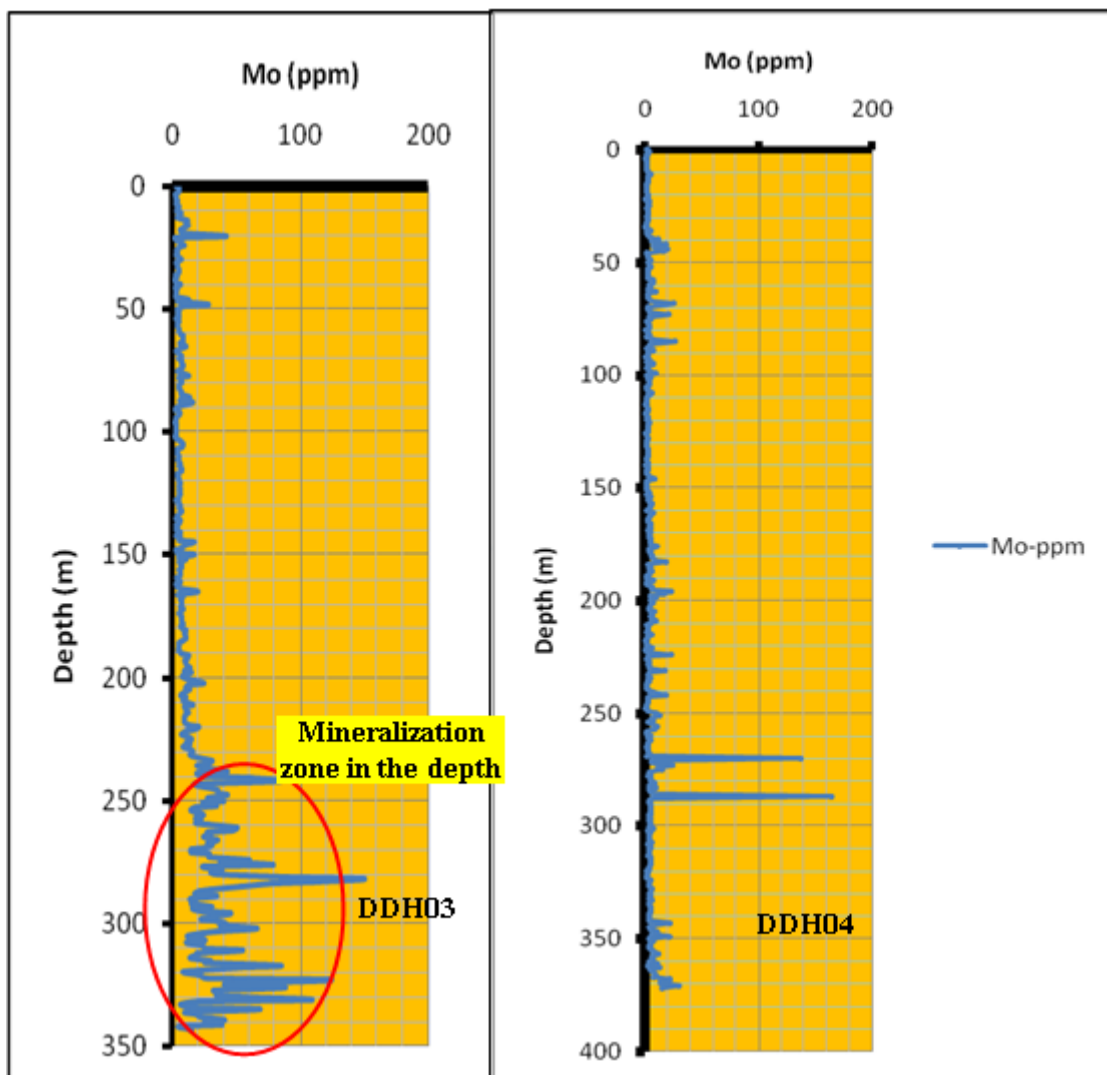


Figure 7. Variations of Mo concentration in DDH03 (inside the anomaly) and DDH04 (outside the anomaly).

4. Conclusions

In this research work, SAFA was utilized to determine the Cu geochemical populations in the frequency domain based on the power-spectrum map. Three geochemical classes were defined by

the power-spectrum thresholds of $10^{12.32}$ and $10^{13.95}$ in the diagram of SAFA. The low-frequency bands for 30 elements were separated using a low-pass filter function based on the threshold of $10^{13.95}$. In the next step, the

low-frequency signals of geochemical data for all of elements were interpreted using PCA. PCA, as a dimension-reduction method, classified the 30 elements into two factors. These results show that the Mo element is in factor 2 as the mineralization phase, and the other 29 elements consisting of Cu and Au were classified in factor 1 as the background component. The Mo geochemical anomaly area related to the low-frequency signals was mapped using the inverse Fourier transformation. This map shows the potential of Mo anomaly in the depth. The deep and the blind mineralizations usually create low-frequency signals in the geochemical distribution map of elements in the surface. The exploratory works such as the boreholes desirably confirm the results of the SAFA-PCA approach in the studied area. The Mo anomaly areas in the depth were properly delineated using the proposed idea. This research work demonstrated that the SAFA-PCA approach could identify the blind and deep geochemical anomaly using the surface geochemical data. This research work shows that there is a relationship between the blind geochemical anomaly and the power spectrum distribution map in FD.

References

- [1]. Yousefi, M. and Carranza, E.J.M. (2017). Union score and fuzzy logic mineral prospectivity mapping using discretized and continuous spatial evidence values. *Journal of African Earth Sciences*. 128: 47-60.
- [2]. Ghezelbash, R., Maghsoudi, A. and Carranza, E.J.M. (2019). An improved data-driven multiple criteria decision-making procedure for spatial modeling of mineral prospectivity: adaption of prediction-area plot and logistic functions. *Natural Resources Research*. pp. 1-18.
- [3]. Zhang, S., Xiao, K., Carranza, E.J.M. and Yang, F. (2019). Maximum Entropy and Random Forest Modeling of Mineral Potential: Analysis of Gold Prospectivity in the Hezuo-Meiwu District, West Qinling Orogen, China. *Natural Resources Research*. 28 (3): 645-664.
- [4]. Ghezelbash, R. and Maghsoudi, A. (2018). A hybrid AHP-VIKOR approach for prospectivity modeling of porphyry Cu deposits in the Varzaghan District, NW Iran. *Arabian Journal of Geosciences*. 11 (11): 275.
- [5]. Shahi, H. and Kamkar Rouhani, A. (2014). A GIS-based weights-of-evidence model for mineral potential mapping of hydrothermal gold deposits in Torbat-e-Heydarieh area. *Journal of Mining and Environment*. 5 (2): 79-89.
- [6]. Konaté, A.A., Pan, H., Khan, N., Keita, O., Cissé, M., Kourouma, M. and Keita, D. (2019). Mineralogy Recognition from In-Situ Elemental Concentration Log Data Using Factor Analysis. In *Petrogenesis and Exploration of the Earth's Interior* (pp. 171-173). Springer, Cham.
- [7]. Afzal, P., Yusefi, M., Mirzaie, M., Ghadiri-Sufi, E., Ghasemzadeh, S. and Daneshvar Saein, L. (2019). Delineation of podiform-type chromite mineralization using Geochemical Mineralization Prospectivity Index (GMPI) and staged factor analysis in Balvard area (southern Iran). *Journal of Mining and Environment*.
- [8]. Gholampour, O., Hezarkhani, A., Maghsoudi, A. and Mousavi, M. (2019). Application of sequential Gaussian simulation and concentration-volume fractal model to delineate alterations in hypogene zone of miduk porphyry copper deposit, SE Iran. *Journal of African Earth Sciences*. 150: 389-400.
- [9]. Ghezelbash, R. and Maghsoudi, A. (2018). Comparison of U-spatial statistics and C-A fractal models for delineating anomaly patterns of porphyry-type Cu geochemical signatures in the Varzaghan district, NW Iran. *Comptes Rendus Geoscience*. 350 (4): 180-191.
- [10]. Parsa, M., Maghsoudi, A., Yousefi, M. and Sadeghi, M. (2017). Multifractal analysis of stream sediment geochemical data: Implications for hydrothermal nickel prospecting in an arid terrain, eastern Iran. *Journal of Geochemical Exploration*. 181: 305-317.
- [11]. Gonçalves, M. A., Mateus, A., Pinto, F. and Vieira, R. (2018). Using multifractal modelling, singularity mapping, and geochemical indexes for targeting buried mineralization: Application to the W-Sn Panasqueira ore-system, Portugal. *Journal of Geochemical Exploration*, 189, 42-53.
- [12]. Afzal, P., Fadakar Alghalandis, Y., Moarefvand, P., Rashidnejad Omran, N. and Asadi Haroni, H. (2012). Application of power-spectrum-volume fractal method for detecting hypogene, supergene enrichment, leached and barren zones in Kahang Cu porphyry deposit, Central Iran. *Journal of Geochemical Exploration*. 112: 131-138.
- [13]. Thiombane, M., Di Bonito, M., Albanese, S., Zuzolo, D., Lima, A. and De Vivo, B. (2019). Geogenic versus anthropogenic behaviour and geochemical footprint of Al, Na, K and P in the Campania region (Southern Italy) soils through compositional data analysis and enrichment factor. *Geoderma*. 335: 12-26.
- [14]. Cao, L. and Cheng, Q. (2012). Quantification of anisotropic scale invariance of geochemical anomalies associated with Sn-Cu mineralization in Gejiu, Yunnan Province, China. *Geochemical Exploration*. 122: 47-54.
- [15]. Shahi, H., Ghavami, R., Rouhani, A.K., Kahoo, A.R. and Haroni, H.A. (2015). Application of Fourier and wavelet approaches for identification of

geochemical anomalies. Journal of African Earth Sciences. 106: 118-128.

[16]. Zuo, R. (2011). Identifying geochemical anomalies associated with Cu and Pb-Zn skarn mineralization using principal component analysis and spectrum-area fractal the Gangdese Belt, Tibet (China). J. Geochemical Exploration. 111: 13-22.

[17]. Shahi, H. (2017). Prediction of dispersed mineralization zone in depth using frequency domain of surface geochemical data. Journal of Mining and Environment. 8 (3): 433-446.

[18]. Shahi, H., Ghavami, R., Kamkar Rouhani, A. and Asadi Haroni, H. (2014). Identification of mineralization features and deep geochemical anomalies using a new FT-PCA approach. Geopersia. 4 (2): 227-236.

[19]. Shahi, H., Ghavami Riabi, R., Kamkar Ruhani, A. and Asadi Haroni, H. (2015). Prediction of mineral deposit model and identification of mineralization trend in depth using frequency domain of surface geochemical data in Dalli Cu-Au porphyry deposit. Journal of Mining and Environment. 6 (2): 225-236.

[20]. Shahi, H., Ghavami, R. and Rouhani, A.K. (2016). Detection of deep and blind mineral deposits using new proposed frequency coefficients method in frequency domain of geochemical data. Journal of Geochemical Exploration. 162: 29-39.

[21]. Cheng, Q., Xu, Y. and Grunsky, E. (2000). Integrated spatial and spectrum method for geochemical anomaly separation. Natural Resources Research. 9 (1): 43-52.

[22]. Cheng, Q., Xu, Y. and Grunsky, E. (1999). Integrated spatial and spectral analysis for geochemical anomaly separation. In: Lippard, S.J., Naess, A., Sinding-Larsen, R. (Eds.), Proceedings of the Fifth Annual Conference of the International Association for Mathematical Geology, Trondheim, Norway 6-11th August, vol. 1. pp. 87-92.

[23]. Cheng, Q. (2006). Multifractal modelling and spectrum analysis of gamma ray spectrometer data from southwestern Nova Scotia, Canada. Science in China. 49 (3): 283-294.

[24]. Dobrin, M.B. and Savit, C.H. (1998). Geophysical prospecting: McGraw-Hill Book Co., New York, 867 P.

[25]. Bhattacharyya, B.K. (1966). Continuous spectrum of the total-magnetic-field anomaly due to a rectangular prismatic body. Geophysics. 31 (1): 97-121.

[26]. Gonzalez, R.C. and Woods, R.E. (2002). Digital image processing. Prentice-Hall, Upper Saddle River, NJ. 793 P.

[27]. Hassani, H., Daya, A. and Alinia, F. (2009). Application of a fractal method relating power spectrum and area for separation of geochemical anomalies from background. Aust J Basic Appl Sci. 3 (4): 3307-3320.

[28]. Grunsky, E.C. (1997). Strategies and methods for the interpretation of geochemical data. In: Current Topics in GIS and Integration of Exploration Datasets, Short Course, Exploration Workshop. 145 P.

[29]. Harris, J.R., Grunsky, E.C. and Wilkinson, L. (1997). Developments in the effective use of litho-geochemistry in regional exploration programs: application of GIS technology, In Proceedings of Exploration, Fourth Decennial International Conference on Mineral Exploration.

[30]. Chandrajith, R., Dissanayake, C.B. and Tobschall, H.J. (2001). Application of multi-element relationships in stream sediments to mineral exploration: a case study of Walawe Ganga Basin, Sri Lanka. Applied Geochemistry. 16 (3): 339-350.

[31]. Garrett, R.G. and Grunsky, E.C. (2001). Weighted sums- knowledge based empirical indices for use in exploration geochemistry. Geochemistry: Exploration, Environment, Analysis. 1 (2): 135-141.

[32]. Davis, J.C. (2002). Statistics and Data Analysis in Geology, 3rd ed. John Wiley & Sons, Inc., New York. 550 P.

[33]. Cheng, Q., Jing, L. and Panahi, A. (2006). Principal component analysis with optimum order sample correlation coefficient for image enhancement. International Journal of Remote Sensing. 27 (16): 3387-3401.

[34]. Cheng, Q., Bonham-Carter, G., Wang, W., Zhang, S., Li, W. and Xia, Q. (2011). A spatially weighted principal component analysis for multi-element geochemical data for mapping locations of felsic intrusions in the Gejiu mineral district of Yunnan, China. Computer & Geosciences. 37: 662-669.

[35]. Yousefifar, S., Harooni, H.A., Karami, J. and Jafari, M.R. (2011). Prospecting of Au and Cu bearing targets by exploration data combination in southern part of Dalli Cu-Au porphyry deposit, central Iran. Archives of Mining Sciences. 56 (1): 21-34.

[36]. Darabi-Golestan, F., Ghavami-Riabi, R. and Asadi-Harooni, H. (2013). Alteration, zoning model, and mineralogical structure considering litho-geochemical investigation in Northern Dalli Cu-Au porphyry. Arabian Journal of Geosciences. 6 (12): 4821-4831.

[37]. Asadi Haroni, H. (2008). First Stage Drilling Report on Dalli Porphyry Cu-Au Prospect, Central Province of Iran, Technical Report.

[38]. Sadeghi, B., Moarefvand, P., Afzal, P., Yasrebi, A.B. and Saein, L.D. (2012). Application of fractal

models to outline mineralized zones in the Zaghia iron ore deposit, Central Iran. *Journal of Geochemical Exploration*. 122: 9-19.

[39]. Cheng, Q., Agterberg, F.P. and Ballantyne, S.B. (1994). The separation of geochemical anomalies from background by fractal methods. *Journal of Geochemical Exploration*. 51: 109-130.

[40]. Cheng, Q. (2005). Multifractal distribution of eigen values and eigenvectors from 2D multiplicative cascade multifractal fields. *Mathematical Geology*. 37: 915-927.

[41]. Carranza, E.J.M. (2008). Geochemical anomaly and mineral prospectivity mapping in GIS. *Handbook of Exploration and Environmental Geochemistry*, vol. 11. Elsevier, Amsterdam.

[42]. Cheng, Q. (2007). Mapping singularities with stream sediment geochemical data for prediction of undiscovered mineral deposits in Gejiu, Yunnan Province, China. *Ore Geology Reviews*. 32: 314-324.

[43]. Cheng, Q. and Zhao, P. (2011). Singularity theories and methods for characterizing mineralization processes and mapping geo-anomalies for mineral deposit prediction. *Geoscience Frontiers*. 2 (1): 67-79.

[44]. Ghezlbash, R., Maghsoudi, A. and Daviran, M. (2019). Combination of multifractal geostatistical interpolation and spectrum–area (S–A) fractal model for Cu–Au geochemical prospects in Feizabad district, NE Iran. *Arabian Journal of Geosciences*. 12 (5): 152.

[45]. Fyzollahi, N., Torshizian, H., Afzal, P. and Jafari, M.R. (2018). Determination of lithium prospects using fractal modeling and staged factor analysis in Torud region, NE Iran. *Journal of Geochemical Exploration*. 189: 2-10.

[46]. Shokouh Saljoughi, B., Hezarkhani, A. and Farahbakhsh, E. (2018). A comparative study of fractal models and U-statistic method to identify geochemical anomalies; case study of Avanj porphyry system, Central Iran. *Journal of Mining and Environment*. 9 (1): 209-227.

شناسایی آنومالی مولیبدن در عمق با استفاده از یک روش جدید بر مبنای تحلیل فرکتالی طیف توان - مساحت

حسین مهدیان‌فر

گروه مهندسی معدن، مجتمع آموزش عالی گناباد، ایران

ارسال ۲۰۱۹/۱/۴، پذیرش ۲۰۱۹/۷/۶

* نویسنده مسئول مکاتبات: hssn.shahi@gmail.com

چکیده:

شناسایی کانی‌سازی پنهان و عمیق با استفاده از داده‌های ژئوشیمیایی سطحی یک موضوع چالشی در اکتشاف مواد معدنی است. در این پژوهش به منظور تشخیص و ترسیم آنومالی پنهان و عمیق مولیبدن در منطقه کانی‌سازی مس - طلا پورفیری دالی یک روش جدید بر مبنای تحلیل فرکتالی طیف توان - مساحت و تحلیل مؤلفه‌های اصلی به کار گرفته شد. کانسار دالی بر روی کمر بند ولکانیک - پلوتونیک سهند بزمان در قسمت مرکزی ایران قرار دارد. داده‌های ژئوشیمیایی با استفاده از تبدیل فوریه به حوزه فرکانس تبدیل شده و روش فرکتالی طیف توان - مساحت به منظور کلاسه‌بندی فرکانس‌های ژئوشیمیایی و تشخیص جوامع ژئوشیمیایی به کار گرفته شده است. سیگنال‌های فرکانسی خیلی پایین در روش فرکتال، با استفاده از تابع فیلتر پایین گذر جدا و با استفاده از روش تحلیل مؤلفه‌های اصلی مورد تفسیر قرار گرفته‌اند. این روش نشان می‌دهد مولیبدن نقش مهمی در فاز کانی‌سازی در سیگنال‌های با فرکانس‌های خیلی پایین که مرتبط با کانی‌سازی عمیق هستند دارد و یک نوآوری جدید در این مطالعه است. سپس نقشه آنومالی ژئوشیمیایی مولیبدن با استفاده از تبدیل فوریه معکوس به دست آمده است. این پژوهش نشان می‌دهد مقادیر بالای طیف توان در روش فرکتالی طیف توان - مساحت مرتبط با عناصر زمینه و کانی‌سازی عمیق هستند. دو گمانه اکتشافی حفر شده در داخل و خارج محدوده آنومالی مولیبدن به خوبی نتایج روش پیشنهادی را تأیید می‌کند.

کلمات کلیدی: تحلیل فرکتالی طیف توان - مساحت، جدایش آنومالی، تحلیل مؤلفه‌های اصلی، آنومالی ژئوشیمیایی پنهان، تشخیص الگو.
